THE ASTROPHYSICAL JOURNAL, 367:141–148, 1991 January 20

SUPERBUBBLE BLOWOUT IN THE GIANT H II REGION NGC 2363?

JEAN-RENÉ ROY[1]
Département de Physique, and Observatoire astronomique du mont Mégantic, Université Laval
J. BOULESTEIX
Observatoire de Marseille
GILLES JONCAS[1]
Département de Physique, and Observatoire astronomique du mont Mégantic, Université Laval
AND
B. GRUNDSETH
Canada-France-Hawaii Telescope Corporation
Received 1990 April 5; accepted 1990 July 18

ABSTRACT

The velocity field of the giant H II complex NGC 2363 in the SBm galaxy NGC 2366 has been mapped in the [O III] λ 5007 Å line using a scanning Fabry-Perot interferometer. The [O III] line profiles correspond to symmetrical and single component profiles in most of the nebulae of NGC 2366, except in the bright core of the giant H II NGC 2363 where strong splitting of the [O III] line occurs. This splitting is consistent with a bubble 200 pc in diameter expanding with a velocity of 45 km s^{-1}. The total kinetic energy of the bubble is 2×10^{52} ergs; the kinematic age of the bubble is less than or equal to 2×10^6 yr. The bubble could be produced by the sole action of combined stellar winds from the central clusters of OB stars. A well-defined sector, 150 pc wide, of the H II complex originating at the bubble shows systematic receding velocities; it is suggested that this region acts as a vent through which gas escapes into the halo of the galaxy. Large Hα shells are observed in the surroundings of NGC 2363. There is also evidence for a very broad and low-intensity [O III] high-velocity ($\sim$1000 km s^{-1}) component associated with the bubble.

Subject headings: galaxies: individual (NGC 2366) — nebulae: H II regions — nebulae: individual (NGC 2363) — nebulae: internal motions

I. INTRODUCTION

Giant H II regions are loci of the interstellar medium undergoing intense bursts of formation of massive stars. It is the scale of star formation that clearly distinguishes giant H II regions from normal objects (Hunter and Gallagher 1985). Giant nebulae are excited by copious amounts of ultraviolet photons ($h\nu > 13.6$ eV) produced in their central parts by superclusters of OB stars totaling 10^3 to 10^5 $M_\odot$ (Kennicutt 1984). The Balmer luminosities of giant H II regions reach 10^{39} to 10^{41} ergs s^{-1} which makes these objects visible even in distant galaxies. Giant extragalactic H II regions (GEHRs) have been surveyed extensively to establish the chemical composition of galaxies, to study star formation, to investigate the spiral structure of galaxies, and to measure distances to galaxies. Despite the widespread use of giant H II regions for tackling fundamental issues of galaxy evolution, surprisingly little is known about their nature and their exciting stars. The difficulties are mostly observational; no comparable objects are known to exist in the Galaxy and one requires access to 4 m class telescopes at excellent sites or to the *Hubble Space Telescope* to study these small angular-size objects in some details.

Star clusters embedded in giant H II regions are among the most luminous stellar aggregates found in galaxies (Kennicutt and Chu 1988). The colossal OB associations or clusters responsible for GEHRs are likely progenitors of sequential supernovae, Wolf-Rayet stars, and other massive stars with powerful stellar winds. These energetic objects will combine with the shearing forces of *champagne* flows in shaping the velocity fields of the giant H II regions. Furthermore, the mechanical energy input from their massive stars could be largely sufficient to expel gas from the parent galaxies (Dekel and Silk 1986). Some of the material expelled from galaxy disks may be seen as giant H I shells (Heiles 1984, 1990) or large H II bubbles (Courtès *et al.* 1987). McCray and Kafatos (1987) and Tenorio-Tagle and Bodenheimer (1988) have reviewed the evidence for giant shells in the galaxies of the Local Group.

A puzzling property of GEHRs is the relationship that exists between the internal velocity dispersions $\langle W \rangle$ of the *first-ranked* H II regions and the absolute blue magnitudes of the parent galaxies (Melnick 1978; Roy, Arsenault, and Joncas 1986). This scaling appears like some sort of Tully-Fisher relation for the ionized gas of galaxies. However, while the physics of the H I gas used in the Tully-Fisher relation is reasonably well understood, we remain at a lost when interpreting the scaling of nebular velocities with galaxian luminosities. The potential for using this parameter of H II regions as an extragalactic distance indicator exists, but remains risky as long as we do not understand the underlying physics.

Velocity dispersions in GEHRs are measured from emission line profiles (e.g., Hα, [O III]) integrated over whole H II regions. Such profiles are obtained with large-aperture Fabry-Perot interferometers; most GEHRs have angular sizes smaller than 45″. The *e*-folding width of the Gaussian profile which, convolved with the thermal broadening function, best reproduces the observed profile is taken as the velocity width. The

[1] Visiting Astronomer, Canada-France-Hawaii Telescope, operated by the National Research Council of Canada, the Centre National de la Recherche Scientifique of France, and the University of Hawaii.

observed widths are supersonic and can reach values as high as 30–40 km s^{-1} (Smith and Weedman 1972). Velocity widths of GEHRs are also correlated with the total line emission fluxes, F(Hα), and diameters of the H II regions (Melnick 1977; Gallagher and Hunter 1983; Roy, Arsenault, and Joncas 1986; Hippelein 1986; Melnick *et al.* 1987; Arsenault and Roy 1988). More recently Arsenault, Roy, and Boulesteix (1990) analyzed those relations from a sample of 88 H II regions in the Virgo spiral galaxy NGC 4321. They found a tight relationship between F(Hα) and W only for the 31 H II regions having the *highest* surface brightness; the other regions did not display any correlation.

However, what is meant by "velocity width" or "dispersion" is actually the sum of radial velocity differences across the face of GEHRs, plus large-scale velocity flows along the lines of sight in the nebula, plus true velocity dispersion. These three effects concur in broadening the line profiles. In order to evaluate the relative importance of these effects and to investigate the origin of supersonic motions in GEHRs, we are carrying out a program of Doppler imaging of giant H II regions in nearby galaxies using a Fabry-Perot interferometer. This paper presents observations of the giant H II region NGC 2363 located in the late-type galaxy NGC 2366. We found that the velocity field of this GEHR is characterized by relatively small differences in radial velocities across its face, by large widths of profiles, and by an expanding central bubble which is associated with possibly very fast gas.

II. OBSERVATIONS

NGC 2366 is a small late-type SBm IV–V dwarf galaxy in the M81 group; its size and shape are reminiscent of the Large Magellanic Cloud, with the giant H II region NGC 2363 standing for 30 Doradus. In its overall properties, NGC 2363 is indeed very similar to 30 Doradus (Kennicutt 1984). A detailed structural study of NGC 2363 has been published by Kennicutt, Balick, and Heckman (1980; hereafter KBH), and Hunter (1982) studied this object as part of her study of star-forming regions in irregular galaxies. The chemistry of NGC 2363 was investigated by Peimbert, Pena, and Torres-Peimbert (1986). We assume a distance modulus of $\mu = 27.10$ (de Vaucouleurs 1979*a*, *b*) which corresponds to a distance of approximately 2.6 Mpc and a scale of 13 pc arcsec^{-1} at the galaxy. KBH derived several physical parameters pertaining to NGC 2363 and assumed a distance of 3.5 Mpc; whenever we use distance-dependent parameters from KBH they will be adjusted for our lower value of distance.

The observations were performed at the f/8 Cassegrain focus of the 3.6 m CFH telescope (Mauna Kea, Hawaii) in 1987 December; we used PALILA which consists of a f/2 focal reducer, a scanning Fabry-Perot interferometer, and a photon counting camera. The focal reducer gives a total field of view of $5' \times 5'$ on the 256×256 pixels of the camera; the field is limited by the detector. The [O III] 5007 Å line was observed through an interference filter centered at 5010 Å with a FWHM of 13 Å. The [O III] line is intrinsically more narrow than Hα; its spectral domain is also relatively free from night-sky emission lines and it is very strong in NGC 2363. The free spectral range of the interferometer (5 Å = 298.8 km s^{-1}) was scanned through 40 scanning steps which yields for each pixel ($1''.2 \times 1''.2$ on the sky) the intensity profile of the [O III] line. Total exposure time was 32,000 s or 800 s per channel spread over three nights.

We used the Hβ line at 4861.33 Å for wavelength calibration. Because the properties of the coatings change with wavelength (Koestler 1960; Lichten 1985), the difference between the interference order at 5007 Å and 4861 Å has some uncertainty which leaves an error of a few km s^{-1} in the zero-point of the radial velocities. The barycenter of the emission line is found with an accuracy better than one sampling step of the interferometer (7.5 km s^{-1}); the effective accuracy in relative velocity for the high S/N profiles is of the order of ± 1 km s^{-1}. The software for reducing the Fabry-Perot data has been developed by one of us (J.B.). More details about the data reduction for Fabry-Perot observations obtained in the scanning mode are given by Laval *et al.* (1987).

III. RESULTS

a) General Velocity Field

Figure 1 (Plate 1) shows an Hα image of the galaxy NGC 2366 resulting from three exposures of 3000 s obtained with the Mont Mégantic Observatory 1.6 m telescope using an RCA 320×512 CCD adapted to a f/8–f/3.5 focal reducer. It was produced by subtracting a continuum image obtained at $\lambda = 7000$ Å ($\Delta\lambda = 200$ Å). NGC 2363 is the largest of the nebular complexes seen at the southwestern tip of the galaxy. Our Fabry-Perot observations correspond to a $5' \times 5'$ field centered on the giant H II regions NGC 2363. The field includes several H II regions; however, our discussion will deal mostly with NGC 2363 which has been divided in the past as two regions, NGC 2366 A and B. Close match between the radio continuum (6 cm) and Hα maps indicate lack of appreciable dust within and near the nebula (KBH). The total Hα flux of A is 10 times larger than B (Kennicutt 1978).

Figure 2 shows the [O III] 5007 map obtained by summing

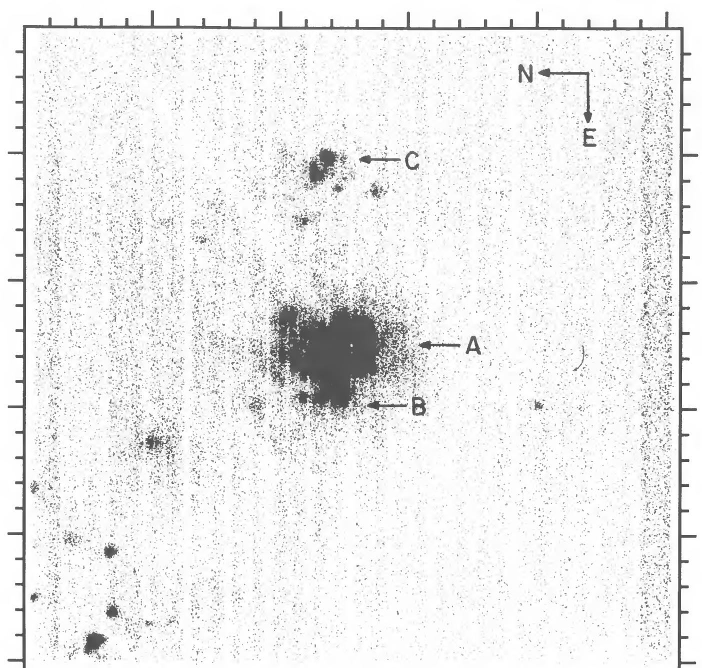

FIG. 2.—[O III] image of the southern half of the galaxy NGC 2366 obtained by summing the 40 steps from the Fabry-Perot scan at the CFHT. The diagonal line is due to a thin wire holding a mask in front of the brightest core to avoid saturation of the photon counting camera. The pixel size on this image is $1''.2$. The field of 256×256 pixel^2 corresponds to approximately $5' \times 5'$.

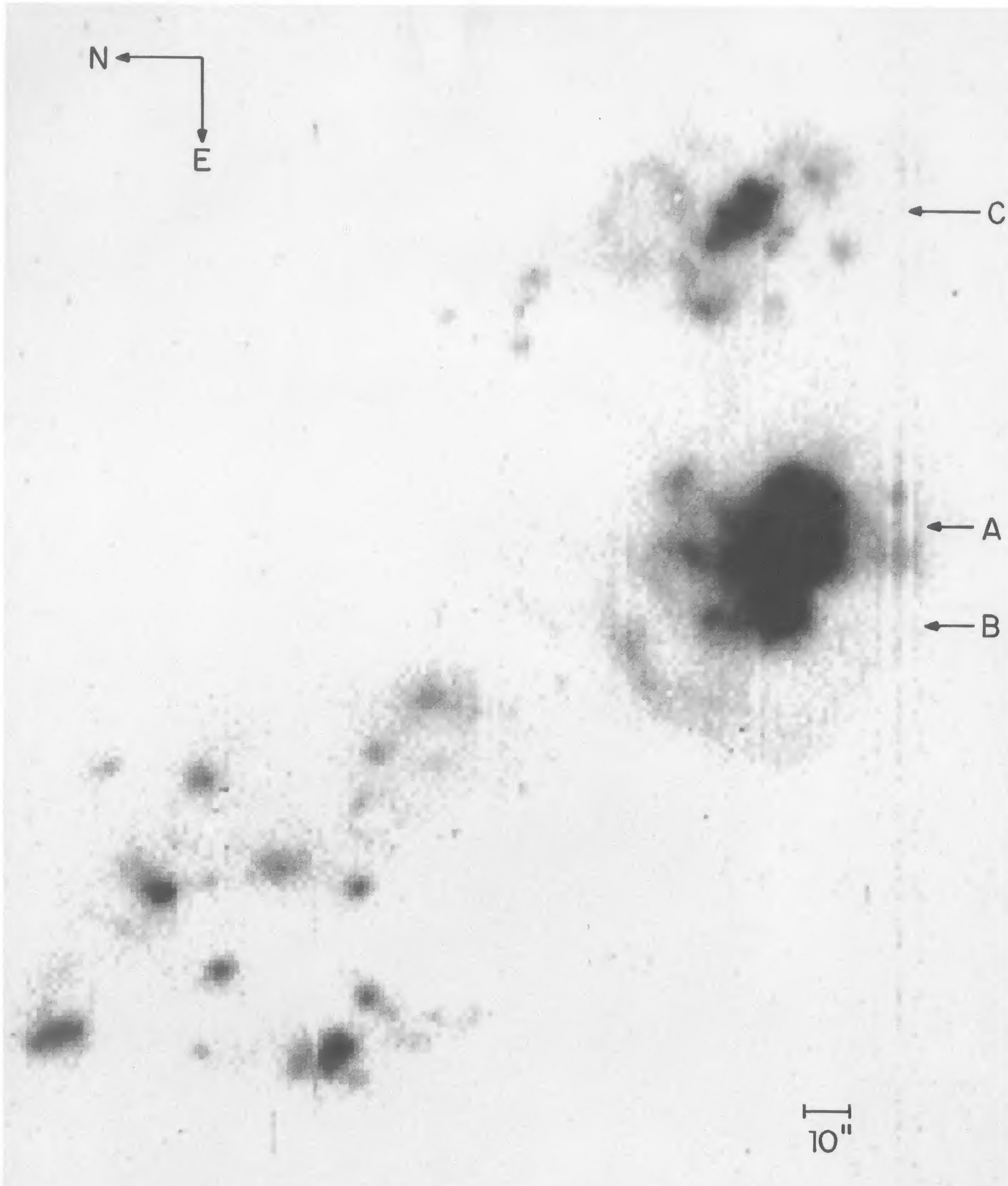

FIG. 1.—Monochromatic Hα CCD image of the southern half of the galaxy NGC 2366 obtained with the 1.6 m telescope of Mont Mégantic Observatory. The largest H II regions, NGC 2366A (NGC 2363), B, and C are identified. The field shown in 218 × 254 pixel^2; pixel size is 1".1. At a distance of 2.6 Mpc, 1" ≈ 13 pc.

ROY, BOULESTEIX, JONCAS, AND GRUNDSETH (*see* **367**, 142) all the Fabry-Perot channels. The image is affected by some cosmetic defects; in particular, the vertical lines of lower sensitivity are due to a misadjustment of the video clock rate of the television system used in the photon counting camera. The line profiles are not affected by the pattern. The diagonal line is caused by a thin wire holding a 1″ mask that we positioned over the brightest part of the core of NGC 2363 (i.e., blob no. 1 in Fig. 1 of KBH) to avoid saturation of the photon counting camera. Seeing and slight shifts of the mask from night to night have allowed some sampling of the bright area, but our photometry of this region is incorrect in [O III]; instead we relied on the Hα image which we calibrated by using the photometry of Kennicutt (1978).

Figure 3 (Plate 2) shows an enlarged section of Figure 1 centered on the H II complex NGC 2363 and its surroundings. The giant H II region itself is built around two bright knots A and B (Fig. 1); each knot may harbor separate stellar associations. The brighter one (peanut-shaped) corresponds to NGC 2366A and the smaller one to the east is NGC 2366B. The squares delineate the areas shown in Figure 4. Figure 4*a* displays for the larger area each individual [O III] line profile normalized to the maximum intensity at each pixel. Each little box corresponds to the integrated [O III] profile of an area encompassing 2 × 2 pixels. Figure 4*b* shows the same for the smaller boxed area of Figure 3, but this time with no binning of the pixels. The horizontal axis of each box represents the wavelength range covered (5 Å = 298.8 km s^{-1}). Although most line profiles appear symmetrical and well-represented by a one-component fit, there are places (e.g., right center) where profiles become broader and asymmetrical and where splitting occurs. Other H II regions and diffuse emission over the 5′ × 5′ field present symmetrical one-component profiles. Depite the fact that NGC 2363 was considered as two regions, A and B, by previous authors, there is no reason to distinguish B from A kinematically.

b) *Expanding Shell Structure*

The most conspicuous feature is at the center where the [O III] profiles display very clear splitting. The region where strong line splitting occurs is centered on the brightest core. A closer view of the [O III] profiles in this area is shown in Figure 5; the area shown is 20″ × 20″ (250 × 250 pc^2). The amount of splitting varies as a function of position, and we interpret it as expanding motion; the velocity difference has a maximum of 90 km s^{-1} at the center and decreases away from it (Fig. 6). The behavior of the split profiles is entirely consistent with an expanding shell about 180 pc (N–S) by 230 pc (E–W) moving at 45 km s^{-1} with respect to its own barycenter (although contraction cannot be ruled out). The radial velocities are consis-

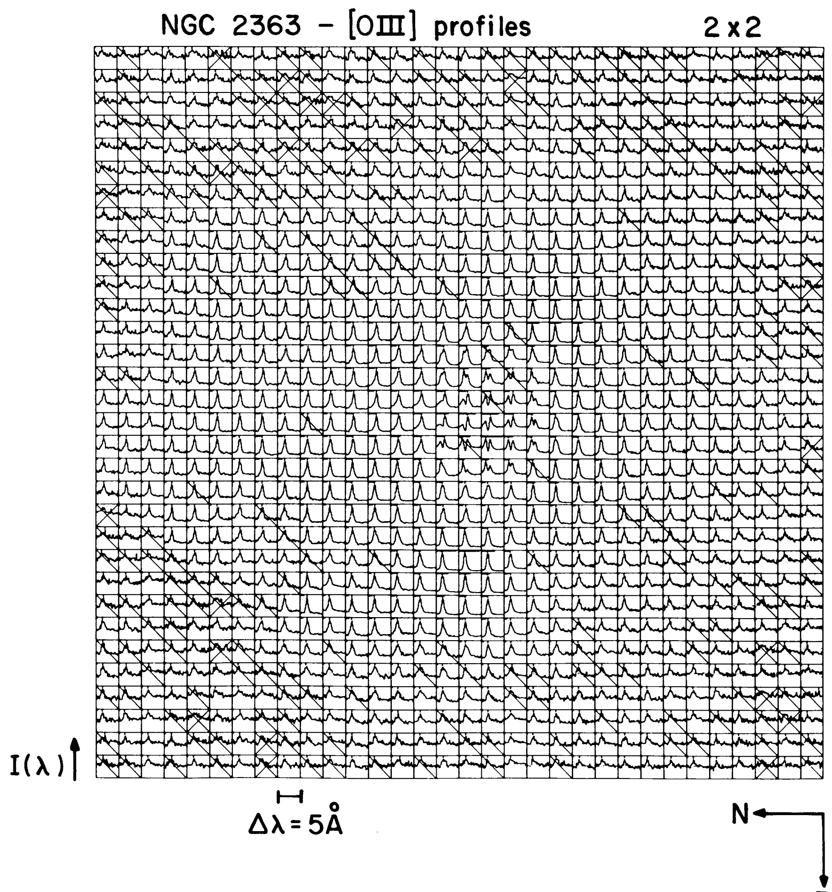

FIG. 4*a*

FIG. 4.—(*a*) [O III] line profiles (binned 2 × 2 pixels) of a 77″ × 77″ field centered on NGC 2363; this corresponds to the larger boxed area in Fig. 3. Each profile is normalized to the maximum count in each bined pixel. The horizontal axis of each box represents the free spectral range of the etalon, i.e., 5 Å = 298.8 km s^{-1}. (*b*) [O III] line profile of a 38″ × 38″ field centered on NGC 2363; no binning was done. This corresponds to the smaller boxed area in Fig. 3.

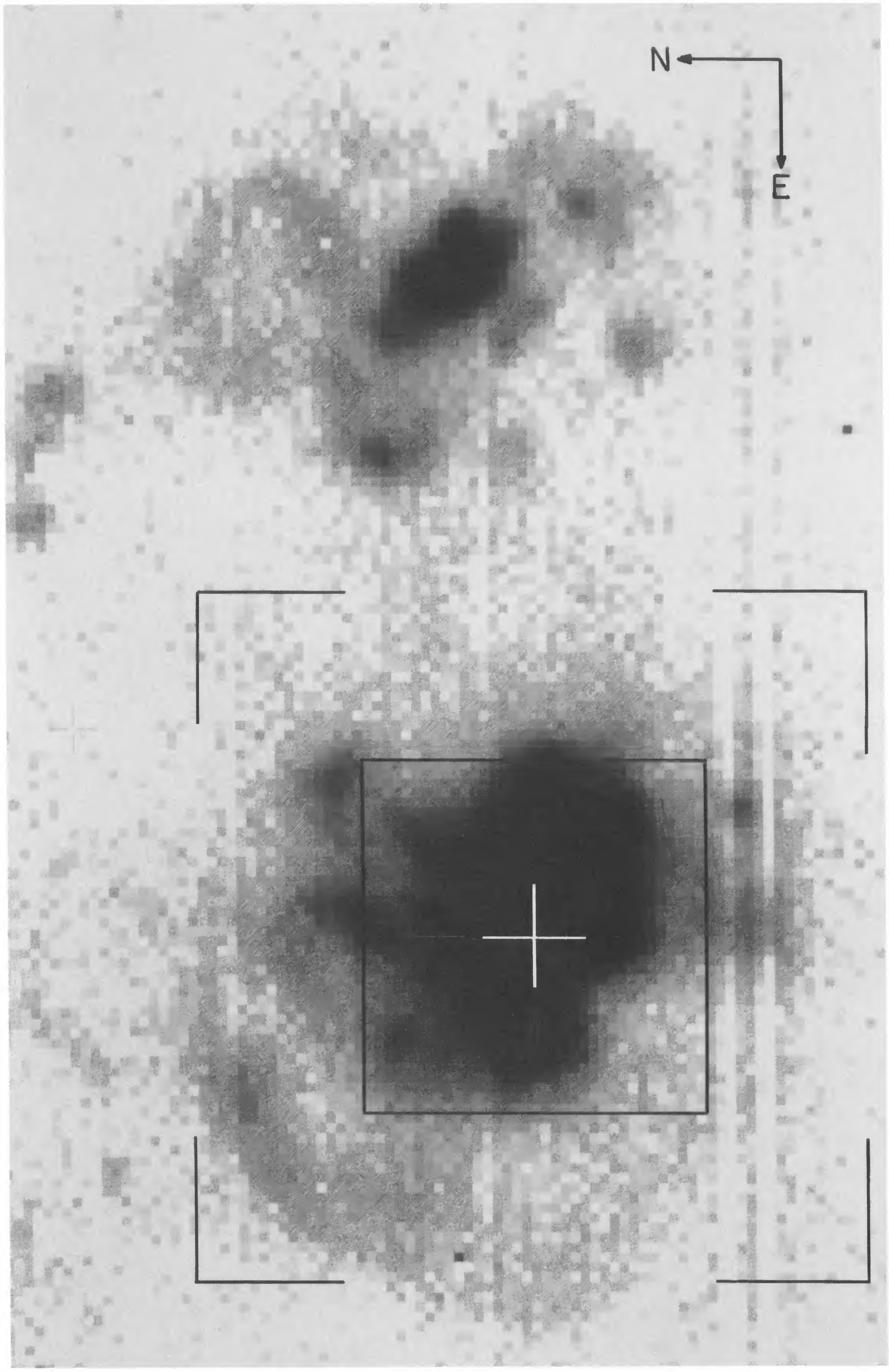

FIG. 3.—Enlarged view of Fig. 1 showing the three largest giant H II regions of NGC 2366 in Hα. This field of view corresponds to an area of 98″ × 153″, or 1274 × 1990 pc^2.

ROY, BOULESTEIX, JONCAS, AND GRUNDSETH (*see* **367**, 143)

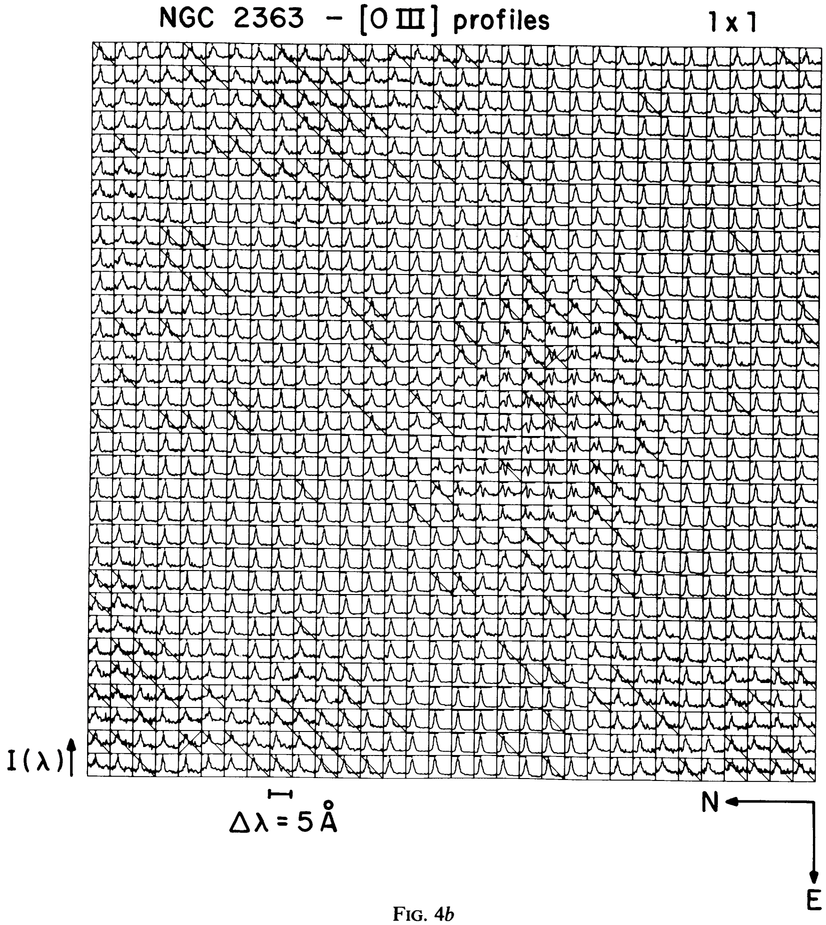

FIG. 4b

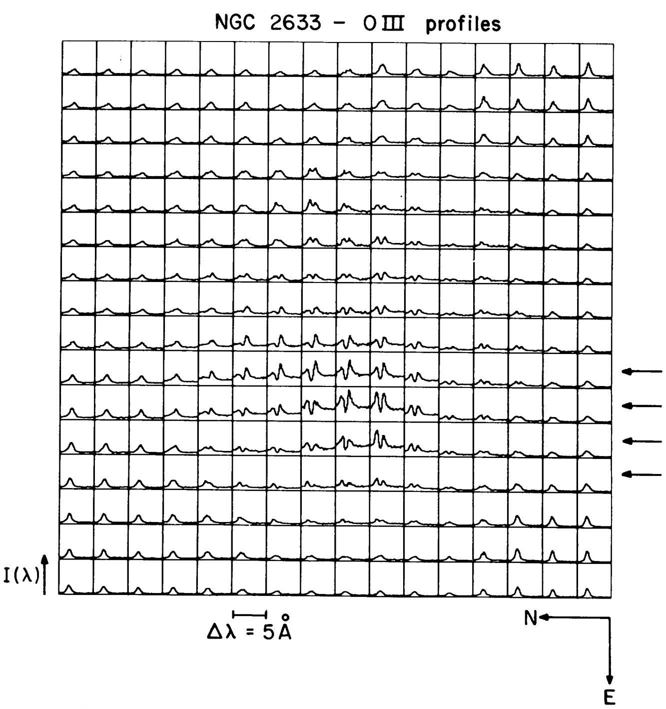

FIG. 5.—Enlarged view of the [O III] line profiles of the area corresponding to the central expanding bubble. The line profile intensities are normalized to that of the brightest pixel.

tent with the integrated profiles measured using large-aperture Fabry-Perot interferometry; using an interferometer with a resolution twice lower, Arsenault and Roy (1986) derived a velocity width of 23 km s^{-1} for the Hα profile; the profiles of NGC 2366 A and B could be adjusted by single Doppler components. It should be noted that because of extended wings, a better fit was obtained with a de Voigt profile than with a Gaussian. However, the velocity mapping provides a view of the internal kinematics that could never had been guessed from the integrated profiles.

c) *Evidence for Very High Velocity Gas*

A striking behavior is seen in several of the split [O III] line profiles (Fig. 5); the central dip goes *deeper* than the apparent continuum; lines with such profiles are marked with arrows in the right margin of Figure 5. Since there are no known underlying stellar absorption features in that spectral range, one is forced to accept that on top of the true continuum (both stellar and nebular) is a very broad [O III] emission feature extending well beyond the free spectral range (5 Å) of the Fabry-Perot etalon. The velocities implied by this broad diffuse emission could reach ≈ 1000 km s^{-1}. The high-velocity gas component is obvious in the split profiles, but its presence cannot be excluded in other areas. Indeed, if the extended wings of the large-aperture profiles measured by Arsenault and Roy (1986) corresponds to this gas, many giant H II regions would have high-velocity gas associated with them. Albeit the very high-velocity gas appears associated with the expanding bubble, the

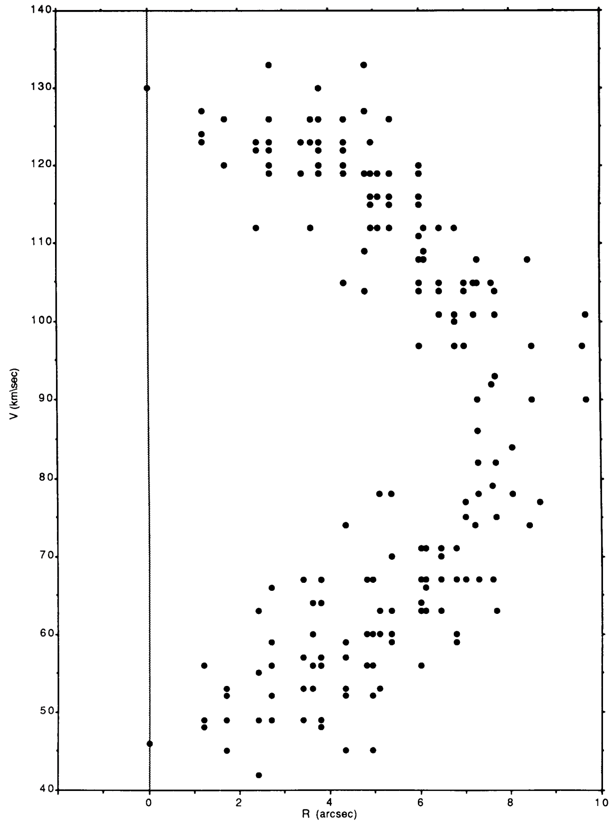

FIG. 6.—Radial velocities measured from the double peaks of the split [O III] line profiles showing the systematic radial behavior consistent with an expanding bubble. The radius is measured from the center of the bubble.

observations cannot specify whether the gas is within or outside the cavity or both.

d) *The "Chimney" of NGC 2366*

Heliocentric radial velocities were derived from the observed shifts of the peaks of the individual line profiles. The general radial velocity map of NGC 2363 reveals an unusual structure (Fig. 7*a*, *b*). The overall fluctuations in radial velocities are rather small, if one excepts the central bubble. There is a general "background" velocity field at about 80–90 km s^{-1}; coming out right from the expanding bubble, a region with velocities higher by about 20–30 km s^{-1} (100–110 km s^{-1}) defines a sector directed north–northwest. This area appears as gas escaping from the central bubble acting as a sort of vent and allowing NGC 2363 to "blow out."

e) *Other* H II *Regions*

Several smaller H II regions were also measured. None of them shows any peculiarity; the profiles are narrow and symmetrical. NGC 2363 is certainly unusual with its expanding bubble.

IV. DISCUSSION

We first summarize the main observational facts which will set the physical constraints on models explaining the velocity field of the giant H II region NGC 2363.

1. The [O III] line profile of the bright core of the giant H II region NGC 2363 is split into two components. The Hα flux emitted from the region corresponding to the expanding bubble represents approximately 60% of the total flux emitted by NGC 2363.

2. The total kinetic energy of the expanding bubble can be calculated assuming $V_{\rm exp} = 45$ km s^{-1}, $R = 100$ pc, and $\langle n \rangle = 10$ cm^{-3}; this density derived by KBH depends only slightly on the geometry of the bubble. Then $E_{\rm kin} \approx 2 \times 10^{52}$ ergs. This energy is of the same magnitude as those of large Galactic or Magellanic supershells observed in H I and Hα (Heiles 1984; Tenorio-Tagle and Bodenheimer 1988).

3. The kinematic age of the bubble is $t \approx R/V_{\rm exp} = 2 \times 10^6$ yr. Because one can expect the expansion to slow with time, the real age of the bubble is probably less than this figure.

4. From the Hα flux one can derive the number of OB stars required to ionize NGC 2363. Scaling for our distance of 2.6 Mpc the luminosity derived by Kennicutt (1984), $L(\mathrm{H}\alpha) = 0.8 \times 10^{40}$ ergs s^{-1} for the whole H II complex of NGC 2363; following a Salpeter initial mass function (IMF) and assuming a solar composition, a total stellar mass of 28,000 $M_\odot$ for OB stars in the range of 10–100 $M_\odot$ is derived (Kennicutt 1983); this is equivalent to the ionizing power of 125 O5 V stars for $N_{\rm Lyman}$(O5 V) $= 5 \times 10^{49}$ s^{-1} (Panagia 1973); it should be remembered that NGC 2366 is a low-metallicity galaxy and that the Lyman photon output depends on the metallicity as $N_{\rm Lyman} \approx Z^{-0.4}$. This means that our OB mass estimate is some sort of upper limit.

5. We interpret the "trough" in the continuum of the split [O III] profiles as due to very high velocity gas present at least along the line of sight of the expanding bubble.

Energy release from massive stars can be in the form of stellar winds, ionizing radiation, or supernova explosions. While in term of total stellar output of energy radiation is dominant, the majority of the kinetic energy input into the interstellar medium comes from supernova explosions due to their high efficiency at transfering energy to the interstellar gas (Abbott 1982). Favored mechanisms to produce large hollow or ring-shaped nebulae are supernova (SN) explosions and stellar winds from OB stars and Wolf-Rayet stars (cf. McKee, van Buren, and Lazareff 1984; Rosado 1986; Dorland, Montmerle, and Doom 1986). Some examples of shells or bubbles caused by the interaction of stellar winds and ionized gas can be found in Lasker (1977), Rosado *et al.* (1981), Goudis, Hippelein, and Münch (1983), Laval *et al.* (1987, 1989). McCray and Kafatos (1987) and Mac Low and McCray (1988) have simulated models involving the combined effects of multiple supernovae exploding in an already existing cavity due to stellar winds from massive stars. Considering the high level of star formation in NGC 2363 and the size and the energy of the bubble in NGC 2363, their model is attractive. McCray and Kafatos have also argued that the effect of low metallicities and large scale height favor the development of supershells in irregular galaxies. However, explaining a particular expanding superstructure is a complicated task as emphasized by the caveats raised by Tenorio-Tagle and Bodenheimer (1988).

Massive stars with powerful winds are likely to be present in NGC 2363. Can stellar winds energize the expanding bubble of NGC 2363? We assume that the stars are concentrated as if they were a single "superstar." The number of stars N_* undergoing a strong stellar wind required to produce the expanding bubble of NGC 2363 of radius $R = 100$ pc, expanding with a velocity of 45 km s^{-1} in a medium of initial density $n_0 = 10$ cm^{-3}, is (Weaver *et al.* 1977: their eqs. [51] and [52])

$$N_* = 3.4 \times 10^{-7} n_0 R^2 V^3 = 3100 \text{ stars} ,$$

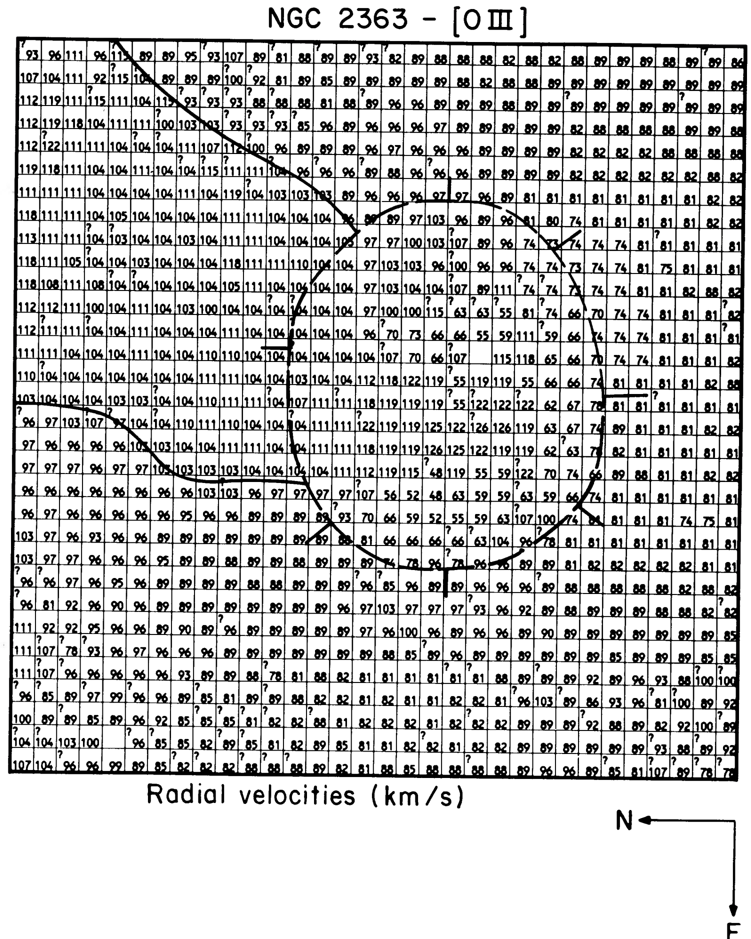

FIG. 7a

FIG. 7.—(*a*) [O III] heliocentric radial velocities of the central 38″ × 38″ of NGC 2363. Wherever the profiles show splitting, only the radial velocities of the strongest component are shown. Question marks indicate two or more peaks of similar intensity. The area corresponding to the expanding bubble is shown by the ellipse. The two irregular lines define the "chimney." (*b*) Gray-scaled map of the [O III] radial velocities which emphasizes the "chimney" or vent of NGC 2363. The total area shown is about 77″ × 70″. The white contour lines are for the [O III] line intensities.

where R is in units of pc and V in km s^{-1}. This equation is based on a mean mechanical luminosity of $\langle L_w \rangle = 10^{36}$ ergs s^{-1} per star. However, the cluster of stars exciting NGC 2363 probably has a rich population of early O and Wolf-Rayet stars, and the mean mechanical energy could be significantly higher than what was inferred above. For example, Dorland, Montmerle, and Doom (1986) have derived the parameters for 45 early-type stars responsible for the excitation of the Carina nebula in our Galaxy, and found $\langle L_w(\text{Carina}) \rangle \approx 8.2 \times 10^{36}$ ergs s^{-1}. If a similar stellar population is present in NGC 2363, 400 O and Wolf-Rayet stars would be required to explain the observed bubble; this is not at all unrealistic. Although large uncertainties affect the derivation of IMF for massive stars and for stars in external galaxies (Lequeux 1985), there could be a sufficient number of massive stars to explain the observed expanding bubble by the sole action of stellar winds.

If stellar winds are able to power expanding bubbles such as the one in NGC 2363, bubbles should be very common. However, NGC 2366 B and C, which are giant H II regions, do not have expanding bubbles in their center. NGC 2366C has a beautiful shell structure visible in the Hα image (Fig. 3); this feature is detected in the [O III] Fabry-Perot observations, but the profiles are not split. Only a few other GEHRs have been observed in detail so far, and the phenomenon does not appear to be common. For example, we have completed the reduction of Fabry-Perot observations of NGC 595 in M33; this GEHR has a Hα luminosity about 4 times smaller than that of NGC 2363; it should still harbor several tens of massive stars in addition to the many Wolf-Rayet stars that it is known to contain (Drissen, Moffat, and Shara 1990). Nevertheless we see no sign of any expanding bubble or shell in NGC 595. Either the mechanical luminosities of early-type stars of NGC 595 and 2363 differ greatly, or some other sources of energy which is more sporadic is at work.

While strong stellar winds are produced by the most massive stars with $M_* > 30$–$50\ M_\odot$ (Lamers 1983), stars with masses as low as 7 $M_\odot$ can become supernovae and are much more numerous. Stellar evolution indicates that we can also expect repeated SN explosions from superclusters of massive stars responsible for the ionization of GEHRs (Tomisaka, Habe, and Ikeuchi 1981; Kolesnik and Silich 1989). Meaburn *et al.* (1989) found that sequential SN as sources of energy and momentum dominate those from stellar winds in the generation of the motions they observed in the large shell N11 in the Large Magellanic Cloud. Stars in the mass range 7–30 $M_\odot$ will be the main contributor to this form of energy input. McCray and

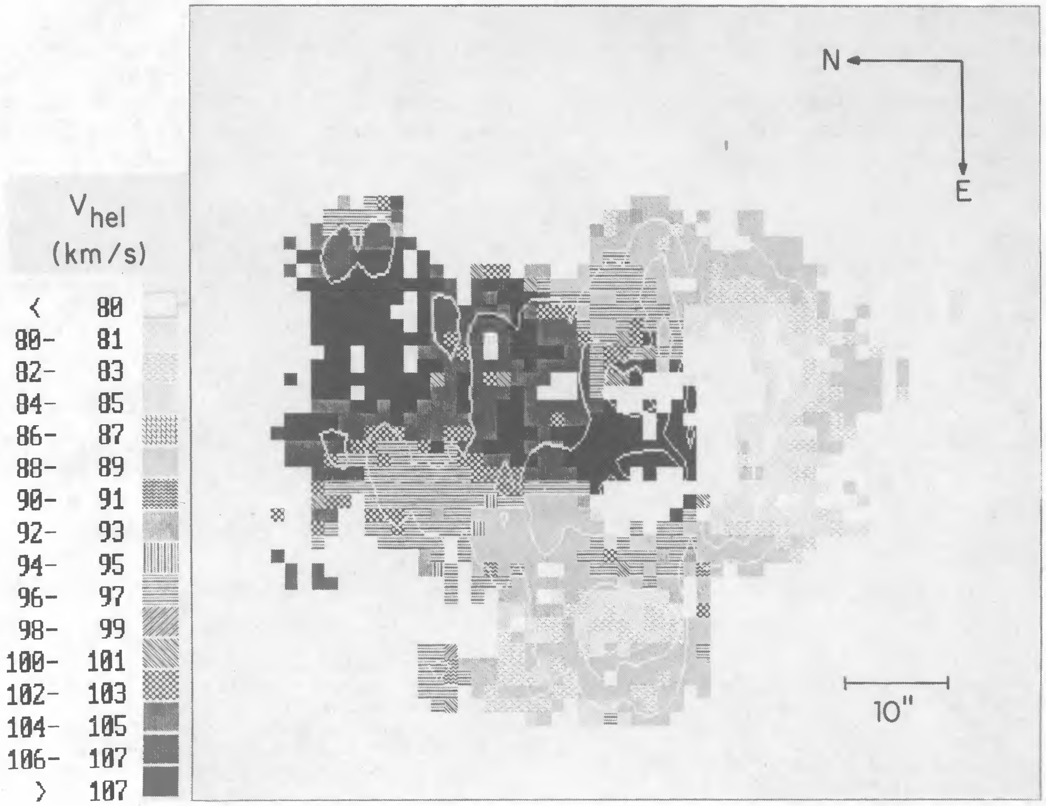

FIG. 7*b*

Kafatos (1987) have treated the sequential supernovae from an evolved OB association like a continuous scale-up wind solution where a constant supernova rate is maintained over the lifetime of the association ($t = 5 \times 10^7$ yr). If we use the kinematic age of 2×10^6 yr as an upper limit to the age of the exciting star cluster, very few stars have had the time to evolve into supernovae. Therefore, this form of mechanical energy input, which will dominate later, is still to come.

Figure 3 shows that NGC 2363 has two "fingers" of brighter material directed roughly northwest which match the redshifted material defining the "vent." The velocity field of NGC 2363 is consistent with venting from the bubble through some sort of chimney effect. That this region acts as a vent through which gas escapes into the halo of the galaxy is also suggested by the presence of several arcs and filaments outside NGC 2363 which reminds Galactic supershells (see Figs. 1 and 3). These Hα shells could represent the remnants of more ancient phases of sequential supernovae in the very active H II regions of NGC 2366. The radial velocities observed across the "venting" region are moderate; they deviate systematically but by a small amount from the general velocity field of the H II region. They are much smaller than those predicted ($\sim$600 km s^{-1}) in the models of superbubble blowout dynamics calculated by Mac Low, McCray, and Norman (1989); the observed velocities are about 10 times smaller than those predicted both in the bubble and in the vent. However, the geometry is not known, and the axis of the "vent" could be close to the plane of the sky.

On the other hand, we have found evidence for very high velocity gas (e.g., $\sim$1000 km s^{-1}) of low surface brightness coinciding at least with the bubble. We cannot exclude the presence of fast gas at other positions across the giant H II region. The higher density and low-velocity expanding bubble could be the interfacing gas pushed by this fast flow. Nevertheless, the precise location of the very fast gas is at the moment difficult to determine. Spectroscopy of NGC 2363 at lower dispersion will help to disentangle the different velocity components, and to determine more accurately the velocity and the location of the very fast gas.

The kinematics of NGC 2363 does not reproduce superbubble blowout dynamics as presented in Mac Low, McCray, and Norman (1989), but is consistent with shells caused by stellar winds and supenovae (cf. Tenorio-Tagle and Bodenheimer 1988). The main characteristic of a blowout is an *acceleration* of the shock moving along the density gradient of a stratified galactic disk. This shock is followed by hot gas from the hot remnant interior which leaks out into the halo of the galaxy. The bubble of NGC 2363 is probably too young. Therefore a preliminary answer to the question in the title is: no, this is not a superbubble blowout. It may become one, but we will have to wait a few millions of years to see it.

V. SUMMARY

Fabry-Perot observations in [O III] and Hα imaging show that the ionized gas of the giant H II regions of the irregular galaxy NGC 2366 is the site of much mechanical energy input. The presence of a large expanding bubble in the center of NGC 2363 can be explained by the energy input of stellar winds from about 400 O and Wolf-Rayet stars. We have also detected a high-velocity gas component ($\approx$1000 km s^{-1} associated with the expanding bubble. The giant H II region NGC 2363 may be in the phase just preceding the breaking out of the high-pressure gas from the H II region into the halo of the galaxy.

We are grateful to Guy Monnet for his competent and enthusiastic support during the observing run at the CFHT. Jean-François Tremblay made useful suggestions. Martin Aubé reduced the CCD frames of NGC 2366 obtained at Mont Mégantic Observatory using IRAF. We are thankful to the referee for catching a significant error, and for providing very helpful comments in the interpretation of the observations. This research was funded in part by the Natural Sciences and Engineering Research Council of Canada.

REFERENCES

Abbott, D. C. 1982, ApJ, 263, 723
Arsenault, R., & Roy, J.-R. 1986, AJ, 92, 567
———. 1988, A&A, 201, 199
Arsenault, R., Roy, J.-R., & Boulesteix, J. 1990, A&A, 234, 23
Clayton, C. A. 1987, MNRAS, 226, 493
Courtès, G., Petit, H., Sivan, J.-P., Dodonov, S., & Petit, M. 1987, A&A, 174, 28
Dekel, A., & Silk, J. 1986, ApJ, 303, 39
de Vaucouleurs, G. 1979a, ApJ, 227, 380
———. 1979b, ApJ, 227, 729
Dorland, H., Montmerle, T., & Doom, C. 1986, A&A, 160, 1
Drissen, L., Moffat, A. F. J., & Shara, M. M. 1990, ApJ, 364, 496
Gallagher, J. S., & Hunter, D. A. 1983, ApJ, 274, 141
Goudis, C., Hippelein, H., & Münch, G. 1983, A&A, 117, 127
Heiles, C. 1984, ApJS, 55, 585
———. 1990, ApJ, 354, 384
Hippelein, H. H. 1986, A&A, 160, 374
Hunter, D. A. 1982, ApJ, 260, 81
Hunter, D. A., & Gallagher, J. S. 1985, AJ, 90, 80
Kennicutt, R. C. 1978, Ph.D. thesis, University of Washington
Kennicutt, R. C. 1983, ApJ, 272, 54
———. 1984, ApJ, 287, 116
Kennicutt, R. C., Balick, B., & Heckman, T. 1980, PASP, 92, 134 (KBH)
Kennicutt, R. C., & Chu, Y. 1988, AJ, 95, 720
Koestler, C. J. 1960, JRes. NBS, 64A, 191
Kolesnik, I. G., & Silich, S. A. 1989, Astrophysics, 30, 178
Lamers, H. J. G. L. M. 1983, in Diffuse Matter in Galaxies, ed. J. Audouze, J. Lequeux, M. Lévy, and A. Vidal-Madjar (Dordrecht: Reidel), 35
Lasker, B. M. 1977, ApJ, 212, 390
Laval, A., Boulesteix, J., Georgelin, Y. P., Georgelin, Y. M., & Marcelin, M. 1987, A&A, 175, 199
Laval, A., Rosado, M., Boulesteix, J., Georgelin, Y. P., Marcelin, M., Greve, A., Larsen, J., & Viale, A. 1989, in Structure and Dynamics of the Interstellar Medium, ed. G. Tenorio-Tagle, M. Moles, and J. Melnick (Heidelberg: Springer), 194
Lequeux, J. 1985, in Birth and Infancy of Stars, ed. R. Lucas, A. Omont, & R. Stora (Amsterdam: North-Holland), 3
Lichten, W. 1985, J. Opt. Soc. Am. A, 2, 1869
Mac Low, M.-M., & McCray, R. 1988, ApJ, 324, 776
Mac Low, M.-M., McCray, R., & Norman, M. L. 1989, ApJ, 337, 141
McCray, R., & Kafatos, M. 1987, ApJ, 317, 190
McKee, F. C., van Buren, D., & Lazareff, B. 1984, ApJ, 258, L115
Meaburn, J., Solomos, N., Laspias, V., & Goudis, C. 1989, A&A, 225, 497
Melnick, J. 1977, ApJ, 213, 15
———. 1978, A&A, 70, 157
Melnick, J., Moles, M., Terlevich, R., & Garcia-Pelayo, J.-M. 1987, MNRAS, 226, 849
Panagia, N. 1973, AJ, 78, 929
Peimbert, M., Pena, M., & Torres-Peimbert, S. 1986, A&A, 158, 266
Rosado, M. 1986, A&A, 160, 211
Rosado, M., Georgelin, Y. P., Georgelin, Y. M., Laval, A., & Monnet, G. 1981, A&A, 97, 342
Roy, J.-R., & Arsenault, R. 1986, ApJ, 302, 579
Roy, J.-R., Arsenault, R., & Joncas, G. 1986, ApJ, 300, 624
Smith, M. G., & Weedman, D. W. 1972, ApJ, 172, 307
Tenorio-Tagle, G., & Bodenheimer, P. 1988, ARAA, 26, 145
Tomisaka, K., Habe, A., & Ikeuchi, S. 1981, Ap&SS, 78, 273
Weaver, R., McCray, R., Castor, J., Shapiro, P., & Moore, R. 1977, ApJ, 218, 377
———. 1977, ApJ, 218, 742

J. Boulesteix: Observatoire de Marseille, 2 Place le Verrier, Marseille F-13248, Cedex 4, France

B. Grundseth: Canada-France-Hawaii Telescope Corporation, P.O. Box 1597, Kamuela, Hawaii 96743

G. Joncas and J.-R. Roy: Département de Physique, Université Laval, Québec, Qc, Canada G1K 7P4